Case Report

Feasibility of Motion Capture-Based Gait Analysis for a Customized Ankle-Foot Orthosis: A Case Report

[Hongwu Wang](#) *

Case Report

Feasibility of Motion Capture-Based Gait Analysis for a Customized Ankle-Foot Orthosis: A Case Report

Hongwu Wang

University of Florida; hongwu.wang@phhp.ufl.edu; Tel.: +1-(352)-2739934

Abstract: This study evaluates the feasibility of employing motion capture technology to assess the biomechanical effects of an ankle-foot orthosis (AFO) with a customized varus control strap on lower-limb kinematics and kinetics during gait. While the biomechanical impacts of hindfoot-posted orthoses are well-documented, the influence of varus corrective strapping on proximal joint mechanics remains underexplored. To address this gap, a single-subject pilot study involving a healthy participant was conducted, with kinematic and kinetic data collected across five walking trials under three conditions: barefoot, shod, and shod+AFO. Results demonstrated that the AFO increased double-limb support time from 15% (barefoot) to 20% (shod+AFO) of the gait cycle and reduced peak ankle plantarflexion and dorsiflexion during the swing phase. Ipsilateral knee extension decreased, while heightened variability in joint moments was observed at the contralateral hip and knee. These findings suggest that varus corrective strapping induces sagittal plane kinematic alterations, with compensatory effects extending to the contralateral limb. This pilot study highlights the utility of motion capture systems in evaluating AFO interventions and underscores the need to assess bilateral biomechanical adaptations. Future research should expand to pathological populations, such as individuals with neuromuscular disorders, and investigate frontal plane mechanics to inform AFO customization for clinical populations.

Keywords: varus corrective strap; ankle-foot orthosis; motion capture analysis; gait biomechanics; subtalar joint control; lower limb kinematics

1. Introduction

The hindfoot, comprising the calcaneus and talus, forms the subtalar joint—a critical articulation with the tibia that enables multiplanar motion essential for gait adaptability and load distribution [1–3]. Dysfunction of this joint is implicated in diverse pathologies, including running injuries, Achilles tendon tears, posterior tibialis tendon dysfunction, and knee osteoarthritis [4–7]. Consequently, subtalar stabilization via orthotic interventions is a cornerstone of treatment for these conditions [8–11].

In a closed kinetic chain (e.g., stance phase of gait), the subtalar joint facilitates motion where the talus and tibia rotate over a relatively fixed calcaneus, allowing the body to adapt to terrain or postural demands [3]. Orthotic strategies targeting this joint often employ hindfoot posting or wedging to modulate alignment and kinetics [12–16]. For example, lateral wedging combined with subtalar strapping has been shown to reduce knee varus moments in medial compartment osteoarthritis, while medial posting mitigates excessive hindfoot eversion in runners [8,14–18]. However, studies examining sagittal plane adaptations report mixed outcomes, with some interventions altering ankle dorsiflexion but sparing proximal joints [16,19]. Systematic reviews further highlight that orthotic effects vary by design, with lateral wedges increasing ankle dorsiflexion and eversion, whereas medial posting reduces eversion moments [20].

Despite these advances, critical gaps persist. First, most research focuses on plantar-surface interventions (e.g., insoles) rather than devices encompassing the leg proximal to the ankle, such as

ankle-foot orthoses (AFOs). Second, while strapping techniques are occasionally combined with wedging for osteoarthritis management [17,18], the isolated effects of subtalar strapping—particularly varus corrective strapping integrated into AFOs—remain unexamined. Traditional AFOs often rely on external dorsal straps for retention, but internal slotted straps could directly apply mediolateral forces to the subtalar joint, potentially enhancing biomechanical efficacy. To date, no studies have quantified the sagittal plane kinematic and kinetic effects of such strapping on the ankle, knee, and hip nor assessed bilateral adaptations.

Motion capture technology, integrated with force plate data, is uniquely suited to address these gaps. Unlike isolated kinetic measurements, motion capture provides high-resolution spatial and temporal data on multi-joint coordination, enabling precise quantification of orthotic-induced adaptations across the kinetic chain [12,16]. This approach is critical for detecting compensatory mechanisms in proximal joints, which may arise from altered subtalar mechanics [12,20]. Furthermore, its ability to synchronize kinematic (e.g., joint angles) and kinetic (e.g., moments) data makes it indispensable for evaluating how AFOs influence both movement patterns and underlying forces.

This study investigates the biomechanical effects of a free-motion AFO with a varus corrective strap on sagittal plane kinematics and kinetics at the ankle, knee, and hip during gait. Using motion capture and force plate analysis, we evaluate bilateral adaptations to address two questions: (1) How does varus strapping alter ankle kinematics and kinetics compared to barefoot and shod conditions? (2) Does subtalar joint correction propagate compensatory changes to ipsilateral or contralateral knee and hip mechanics? Findings will inform the design of AFOs for pathologies requiring subtalar control and underscore the utility of motion capture in orthotic assessment.

2. Materials and Methods

2.1. Subject and AFO Design

A healthy 29-year-old female (height: 1.58 m, weight: 54.43 kg, BMI: 21.8 kg/m²) with no history of orthopedic or vestibular impairments participated in this study. Written informed consent was obtained in accordance with institutional ethical guidelines.

A custom articulated AFO was fabricated for the left limb using 3/16" polypropylene. The design prioritized subtalar joint control while preserving sagittal plane mobility. A certified orthotist performed a plaster cast of the left leg with the calcaneus in neutral alignment. Positive model rectification was conducted by an orthotic resident (3 years of experience), followed by vacuum forming by a certified prosthetics and orthotics technician (CPO). The AFO incorporated Tamarack Flexure Joints® (Tamarack Habilitation Technologies, MN, USA), selected for their clinical prevalence and ability to permit free dorsiflexion (unrestricted) and controlled plantarflexion (20° limit). To minimize skin irritation, foam padding was added at the malleoli, and a posterior heel cut-out was included to facilitate calcaneal motion tracking (Figure 1).

Figure 1. Varus corrective strap.

The key innovation was a varus corrective strap (1″ Velcro®) routed from the lateral AFO shell through an internal slot posterior and inferior to the medial malleolus, applying direct mediolateral force to the subtalar joint (Figure 2). The left shoe was modified with a heel cut-out to enable calcaneal marker visibility during motion capture [21].

Figure 2. Calcaneal cut-out 2.5cm at the widest point and 2.5cm tall.

2.2. Motion Capture and Kinetic Data Acquisition

Kinematic data were collected using a 12-camera Qualisys™ system (Qualisys AB, Sweden; sampling rate: 120 Hz) synchronized with four AMTI™ force plates (Advanced Mechanical Technology Inc., MA, USA; sampling rate: 1 kHz). A total of 56 retroreflective markers were placed bilaterally on lower extremity anatomical landmarks, including the pelvis (L3 spinous process) and feet. Marker placement followed the Oxford Foot Model (OFM) [23–25] for the foot/ankle complex (11 markers per foot), enabling multi-segment foot tracking [26–28]. For the shod and shod+AFO conditions, foot markers were repositioned on shoe surfaces at approximate anatomical locations.

Before dynamic trials, a static calibration trial was captured to generate a subject-specific skeletal model in Visual3D™ (C-Motion, MD, USA). Dynamic trials involved the subject walking self-paced across a 7.6 m walkway (five trials per condition: barefoot, shod, shod+AFO). Marker trajectories and (ground reaction forces) GRFs were synchronized and processed in Qualisys™ Track Manager.

2.3. Outcome Measures

Spatiotemporal, kinematic, and kinetic parameters were analyzed using Visual3D™ (v6.01, C-Motion) and custom MATLAB® (MathWorks, MA, USA) scripts. Spatiotemporal measures included:
- gait speed: stride length/stride time [22].
- stride length/time: heel strike to ipsilateral heel strike.
- stance/swing phase: heel strike to toe-off (stance), toe-off to heel strike (swing).
- double support duration: time with bilateral ground contact.
  Joint angles (ankle, knee, hip) were computed as segment orientations:
- Ankle: foot relative to shank.
- Knee: shank relative to thigh.
- Hip: thigh relative to trunk.
  Net joint moments were derived via inverse dynamics using GRFs and segment kinematics [22]. Moments reflect the net muscular torque at each joint, normalized to body weight.

2.4. Experimental Protocol

Markers were applied bilaterally using the OFM [23–25], with additional proximal markers up to the pelvis (Figure 3). After barefoot trials, foot markers were transferred to shoes. During shod-to-

shod+AFO transitions, malleolar and left calcaneal markers were adjusted to accommodate the AFO. Static and dynamic calibrations preceded each condition to ensure model consistency.

Figure 3. Reflective marker placement for barefoot and shod with AFO conditions.

An additional 34 markers were placed up to the pelvis, including the L3 marker (Figure 3). The markers on the foot were removed after the barefoot condition and replaced on the shoe at approximate positions. The malleoli markers on both legs and the calcaneus marker on the left were removed and replaced during the transition between the shod and shod with AFO conditions. A standing calibration was conducted with the subject static and dynamic before each condition. After the calibration, the subject performed five self-paced walking trials under three conditions: barefoot, shod, and shod with AFO.

2.5. Data Analysis

Raw marker trajectories and GRFs were filtered using a 4th-order Butterworth low-pass filter (cutoff: 6 Hz for kinematics, 50 Hz for kinetics). Gait events (heel strike/toe-off) were identified using a 20 N GRF threshold. Joint angles and moments were time-normalized to 100% of the gait cycle. Descriptive statistics (mean ± SD) were calculated across five trials per condition.

3. Results

3.1. Spatiotemporal

The step length, step time, stance time, and swing time largely remained unchanged (Table 1). There was an overall reduction in speed in the AFO trials (1.258m/s) compared to shod (1.407m/s) and barefoot (1.383m/s) (Table 2). The main spatiotemporal deviation occurs with double limb support in the shod with AFO condition. The double limb support time increased compared to the barefoot condition. The time spent in double support for barefoot is 0.139(+/-0.013s), and the time spent in double support for the AFO condition is 0.206 (+/-0.030s). Stride width remained stable across conditions (0.119–0.147 m).

Table 1. Gait parameters of the left and right sides in each testing condition.

Condition	Side	Step length (m)	Step time (s)	Stance time (s)	Swing time (s)	Initial DBL Support (s)

Barefoot	Left	0.645 ±0.020	0.470 ±0.010	0.539 ±0.012	0.401 ±0.008	0.069 ±0.008
	Right	0.659 ±0.015	0.469 ±0.012	0.540 ±0.015	0.401 ±0.007	0.070 ±0.005
Shod	Left	0.683 ±0.018	0.494 ±0.009	0.591 ±0.010	0.391 ±0.010	0.106 ±0.014
	Right	0.705 ±0.017	0.490 ±0.011	0.602 ±0.010	0.384 ±0.006	0.103 ±0.006
Shod with AFO	Left	0.644 ±0.047	0.502 ±0.050	0.619 ±0.016	0.406 ±0.011	0.095 ±0.016
	Right	0.656 ±0.035	0.519 ±0.045	0.604 ±0.047	0.425 ±0.049	0.111 ±0.014

Table 2. Spatiotemporal gait parameters for the three conditions.

Condition	Speed (m/s)	Stride width (m)	Stride length (m)	Dbl Limb Support (s)
Barefoot	1.383	0.119 ±0.011	1.302 ±0.031	0.139 ±0.013
Shod	1.407	0.142 ±0.016	1.387 ±0.027	0.210 ±0.020
Shod with AFO	1.258	0.147 ±0.013	1.287 ±0.067	0.206 ±0.030

3.2. Kinematics

During the shod with AFO trials, the plantarflexion peak angle decreased on both the left and right sides (Figure 4). During the loading response, the plantarflexion angle on the left increased compared to the barefoot and shod conditions. The peak dorsiflexion angle decreased on the left during the swing phase for the shod with AFO trials. During the midswing on the right, the dorsiflexion angle was reduced compared to the barefoot condition. However, it continued to dorsiflex in preparation for the heel strike, while the barefoot condition decreased into slight plantar flexion.

Knee extension angles decreased throughout most stances for the left AFO condition (Figure 4). The right-side knee angles were relatively uniform across all three conditions. The peak knee extension angles bilaterally for all conditions were larger than normative values [30]. The mean knee extension angle for the left side in each condition was as follows: barefoot -11.19 (0.09)°, shod -11.92 (0.96)°, shod with AFO -14.25 (1.08)°. The mean knee extension angle for the right side was as follows -15.04 (0.40), shod -15.19 (0.77), shod with AFO -13.25 (0.51), while normal knee extension is a maximum of approximately -1° [30].

The left hip angle during the shod with AFO trials demonstrated decreased flexion for the first 15% of the gait cycle, where the angle changes from flexion to extension, then the left hip depicts a greater extension at an earlier percentage of the gait cycle than the barefoot or shod condition (Figure 4). The left peak hip flexion angle is slightly greater than the other two conditions. The right hip peak extension angle for the shod with AFO condition is decreased, while the peak flexion angle is increased, compared to the shod and barefoot trials. Similarly to the knee, the hip peak extension angles for all three conditions were depicted as much greater than the normal range of approximately -2° to -15° [30]. In addition, the transition from flexion to extension during stance on both limbs was

achieved earlier (at 15-20% of the gait cycle) for all three conditions compared to the normal 30-40% of the gait cycle [30].
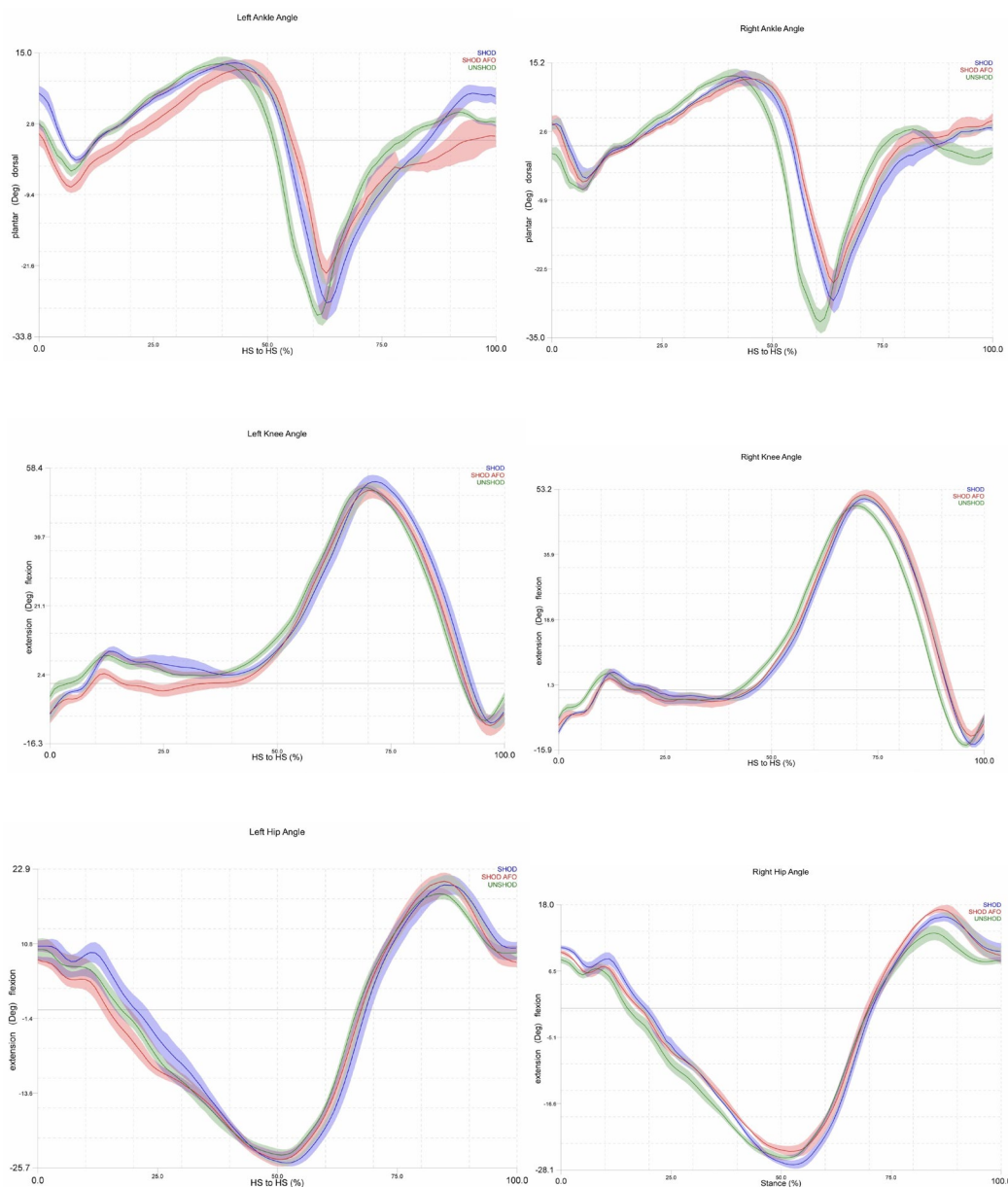

Figure 4. Left and right ankle, knee, and hip angles throughout the gait cycle.

3.3. Kinetics

Overall, greater variances in joint moment were observed in the bilateral hip and knee, with the right side being more impacted than the left during the shod with AFO trial. Additionally, notable results during this trial for joint moments were a lack of knee and hip flexion moments during most of the gait cycle after the loading response, indicating a reduced response of the hamstrings and hip flexors. Similarly, the ankle moments did not follow normative patterns in that they maintained a dorsiflexion moment until approximately 30% of the gait cycle instead of 10%, and the plantarflexion moment occurred at 80% instead of 50% [31]. There was not a span of a neutral or zero moment, as is typically seen in normal gait.

At the hip, the AFO and shod conditions exhibited no extension moment at initial contact, though it was observed in barefoot condition. A reduced flexion moment was observed at the hip during loading response in the AFO and shod trials compared to the barefoot trials. Both hip extension moment peaks occur at about 80% of the gait cycle, whereas normal peak extension

moment occurs during the loading response. In addition, the hip extensor moment magnitudes are greater in this study [left: barefoot 3.44 (0.33)N*m/Kg, shod 3.53 (1.49), AFO 3.10 (0.26); right: barefoot 5.56 (1.43), shod 4.74 (0.29), AFO 1.68 (0.11)] than normal [31]. At the knee, there were also higher extension moment magnitudes than the normal [31].

The AFO trials demonstrated reduced peak knee flexion and extension moments on the right side compared to barefoot and shod. The left side shows similar peak magnitudes, between 20 and 25% of the gait cycle, within the three conditions. However, the AFO trials demonstrated a quicker reduction in extension moment at the knee and level out at a greater extension moment than the other two conditions. Normal gait has four transitions between flexion and extension moments. However, the AFO trials only mirror the transition at the beginning, around 7% of the gait cycle, during the loading response.

All three conditions follow normative graphs for vertical GRF during walking, however, only the barefoot condition exhibits the spike in amplitude shortly after initial contact. The first peak of the left side of GRF (loading response) is delayed in the AFO and shod conditions compared to the barefoot condition (Figure 5). In addition, the second peak (toe-off) was reduced in the AFO and shod conditions compared to barefoot. On the right, there was less of a difference in the percentage of the stance phase in which the initial peak occurs (Figure 5). The toe-off peak was also reduced in magnitude for the shod and AFO conditions compared to barefoot on the right side.
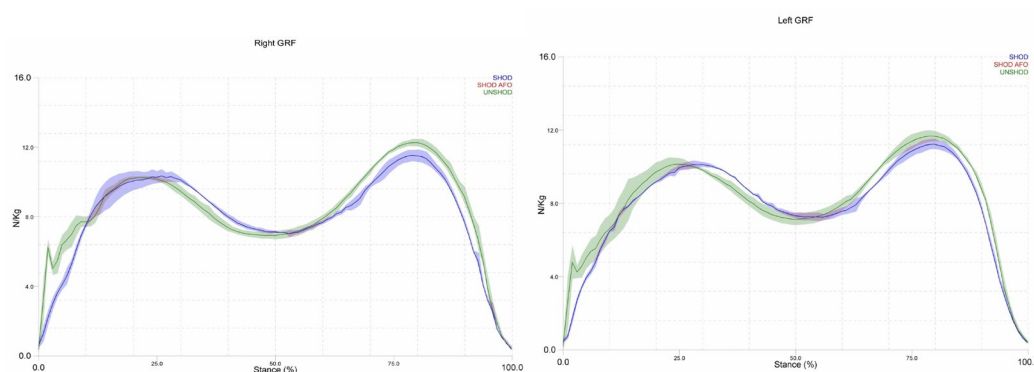

Figure 5. Left and right vertical Ground Reaction Forces throughout the stance phase of gait.

4. Discussion

This study explored the biomechanical effects of a varus corrective strap integrated into an articulated AFO on lower-limb kinematics and kinetics during gait. Contrary to our hypothesis—that the strap would mimic the sagittal plane effects of medial wedging (e.g., increased ankle dorsiflexion and knee extension moments) [16,19]—the strap induced distinct adaptations, highlighting unique mechanisms of subtalar joint control. Below, we contextualize key findings, discuss clinical implications, and address limitations.

4.1. Ankle Kinetics and Kinematics

The AFO with varus strapping reduced peak vertical GRFs during toe-off, consistent with diminished ankle plantarflexion angles and moments. This contrasts with studies of lateral wedges, which increased ankle dorsiflexion [16,20] and suggests that direct mediolateral force application via strapping may alter sagittal plane mechanics differently than plantar-surface interventions. The unrestricted Tamarack joints likely permitted compensatory strategies, such as reduced push-off intensity, to mitigate instability—a phenomenon observed in patients adapting to new orthoses [29]. These findings underscore the need to evaluate AFO designs not only for joint restriction but also for unintended kinetic trade-offs.

4.2. Contralateral Joint Adaptations

Notably, the contralateral (right) limb exhibited increased variability in hip and knee moments during AFO use, a finding absent in studies of bilateral orthotic interventions [17,18]. This asymmetry may reflect compensatory mechanisms to stabilize the pelvis or accommodate altered propulsion from the braced limb. For instance, reduced ipsilateral hip extension moments at heel strike could diminish gluteal engagement, potentially predisposing users to secondary musculoskeletal imbalances (e.g., low back pain) [30]. Such unilateral effects are critical in pathologies like stroke or unilateral osteoarthritis, where contralateral compensations exacerbate injury risk [31]. Future work should prioritize bilateral analyses to capture full-body adaptations to unilateral orthoses.

4.3. Knee Joint Mechanics

While lateral wedging increases early-stance knee extension moments [19], the AFO condition produced no such change. Instead, knee extension moments plateaued at higher magnitudes from mid-stance to pre-swing, suggesting prolonged quadriceps activation. This pattern diverges from the typical flexion-extension moment transition in late stance [32] and may indicate co-contraction of knee flexors (e.g., hamstrings) to counteract instability induced by the AFO. Surface electromyography (EMG) is warranted to clarify muscular coordination strategies during AFO use.

4.4. Gait Speed and Stability

The inverse relationship between gait speed and double-limb support [32] was disrupted in the shod condition, which exhibited the fastest speed (1.407 m/s) yet the highest double-support time (21%). This anomaly may reflect footwear-induced gait adjustments (e.g., rigid soles altering propulsion). Conversely, the AFO condition's slower speed and prolonged double support (20%) align with the literature on orthotic unfamiliarity in healthy users [33]. Longitudinal studies are needed to determine whether prolonged AFO use improves gait efficiency or perpetuates compensatory patterns.

4.5. Feasibility of Motion Capture for Customized AFO Assessment

Motion capture technology demonstrated robust feasibility for evaluating the biomechanical effects of AFOs, particularly in capturing multi-joint adaptations across the kinetic chain. By synchronizing kinematic and kinetic data, the system enabled precise quantification of sagittal plane alterations at the ankle, knee, and hip—critical for understanding how subtalar joint interventions propagate proximally. The integration of force plates provided actionable insights into ground reaction forces and joint moments, revealing compensatory mechanisms (e.g., contralateral variability) that simpler systems (e.g., pedobarography) might overlook. However, challenges such as marker placement consistency, especially during transitions between barefoot, shod, and AFO conditions—and artifacts from reflective footwear highlight the need for standardized protocols to improve reliability. Despite these limitations, motion capture's ability to resolve temporal-spatial gait parameters, coupled with inverse dynamics modeling, underscores its value as a gold standard for orthotic research. Future advancements in markerless systems or hybrid approaches (e.g., combining inertial sensors) could further enhance the practicality of clinical AFO tuning while retaining analytical rigor [12,16,34].

4.6. Limitations

This pilot study has several limitations. First, the single-subject design limits generalizability, particularly to pathological populations who may respond differently to AFOs. Second, marker placement inconsistencies—especially between barefoot and shod conditions—may have introduced kinematic inaccuracies, as evidenced by implausible knee hyperextension values (-12.45°). While the OFM improves foot kinematics [23–25], shoe-mounted markers can underestimate calcaneal motion [34]. Despite heel cut-outs, reflective shoe artifacts compromised calcaneal tracking, necessitating

trial exclusions. Future studies should use non-reflective footwear and assess inter-rater marker placement reliability [33].

5. Conclusions

The varus corrective strap induced sagittal plane biomechanical adaptations distinct from traditional wedging, underscoring the need to evaluate orthotic mechanisms holistically—beyond plantar-surface interventions. Motion capture technology proved feasible and invaluable for this purpose, enabling precise, multi-joint analysis of kinematic and kinetic adaptations across the kinetic chain. Its capacity to synchronize ground reaction forces with joint angles and moments revealed critical insights, such as contralateral joint variability and prolonged knee extensor demands, which would remain undetected with isolated gait measures. However, technical challenges, including marker placement inconsistencies and reflective footwear artifacts—highlight the need for standardized protocols to enhance reliability in heterogeneous cohorts. Future integration of markerless systems or hybrid sensor arrays could mitigate these limitations while retaining motion capture's analytical rigor. These advancements, paired with EMG integration, will further solidify motion capture's role as a gold standard for AFO assessment, bridging research and clinical practice to optimize orthotic designs for subtalar pathologies.

Abbreviations

The following abbreviations are used in this manuscript:

AFO	ankle-foot orthosis
CPO	certified prosthetics and orthotics technician
EMG	electromyography
GRFs	ground reaction forces
OFM	Oxford Foot Model

References

1. Krähenbühl N, Horn-Lang T, Hintermann B, Knupp M. The subtalar joint: a complex mechanism. EFORT Open Rev. 2017;2(7):309-16. doi:10.1302/2058-5241.2.160050
2. Jastifer JR, Gustafson PA. The subtalar joint: biomechanics and functional representations in the literature. Foot Edinb. 2014;24(4):203-9. doi:10.1016/j.foot.2014.06.003
3. Neumann DA, Kelly ER, Kiefer CL, Martens KA, Grosz CM. Kinesiology of the musculoskeletal system. 2nd ed. St. Louis: Elsevier; 2010. p. 585-7.

4. Munteanu SE, Barton CJ. Lower limb biomechanics during running in individuals with achilles tendinopathy: a systematic review. J Foot Ankle Res. 2011;4:15. doi:10.1186/1757-1146-4-15

5. Carr JB 2nd, Yang S, Lather LA. Pediatric Pes Planus: A State-of-the-Art Review. Pediatrics. 2016;137(3):e20151230 . doi:10.1542/peds.2015-1230

6. Levinger P, Menz HB, Fotoohabadi MR, Feller JA, Bartlett JR, Bergman NR. Foot posture in people with medial compartment knee osteoarthritis. J Foot Ankle Res. 2010;3:29. doi:10.1186/1757-1146-3-29

7. Houck JR, Neville CG, Tome J, Flemister AS. Ankle and foot kinematics associated with stage II PTTD during stance. Foot Ankle Int. 2009;30(6):530-9. doi:10.3113/FAI.2009.0530

8. Mündermann A, Nigg BM, Humble RN, Stefanyshyn DJ. Foot orthotics affect lower extremity kinematics and kinetics during running. Clin Biomech Bristol Avon. 2003;18(3):254-62. doi:10.1016/s0268-0033(02)00186-9

9. Wilson F, Walshe M, O'Dwyer T, Bennett K, Mockler D, Bleakley C. Exercise, orthoses and splinting for treating Achilles tendinopathy: a systematic review with meta-analysis. Br J Sports Med. 2018;52(24):1564-74. doi:10.1136/bjsports-2017-098913

10. Parkes MJ, Maricar N, Lunt M, et al. Lateral wedge insoles as a conservative treatment for pain in patients with medial knee osteoarthritis: a meta-analysis. JAMA. 2013;310(7):722-30. doi:10.1001/jama.2013.243229

11. Neville C, Lemley FR. Effect of ankle-foot orthotic devices on foot kinematics in Stage II posterior tibial tendon dysfunction. Foot Ankle Int. 2012;33(5):406-14. doi:10.3113/FAI.2012.0406

12. Karandikar N, Vargas OO. Kinetic chains: a review of the concept and its clinical applications. PM R. 2011;3(8):739-45. doi:10.1016/j.pmrj.2011.02.021

13. Shimada S, Kobayashi S, Wada M, et al. Effects of disease severity on response to lateral wedged shoe insole for medial compartment knee osteoarthritis. Arch Phys Med Rehabil. 2006;87(11):1436-41. doi:10.1016/j.apmr.2006.08.018

14. MacLean C, Davis IM, Hamill J. Influence of a custom foot orthotic intervention on lower extremity dynamics in healthy runners. Clin Biomech Bristol Avon. 2006;21(6):623-30. doi:10.1016/j.clinbiomech.2006.01.005

15. MacLean CL, Davis IS, Hamill J. Short- and long-term influences of a custom foot orthotic intervention on lower extremity dynamics. Clin J Sport Med. 2008;18(4):338-43. doi:10.1097/MJT.0b013e31815fa75a

16. Kuroyanagi Y, Nagura T, Matsumoto H, et al. The lateral wedged insole with subtalar strapping significantly reduces dynamic knee load in the medial compartment gait analysis on patients with medial knee osteoarthritis. Osteoarthritis Cartilage. 2007;15(8):932-6. doi:10.1016/j.joca.2007.02.004

17. Toda Y, Segal N, Kato A, Yamamoto S, Irie M. Effect of a novel insole on the subtalar joint of patients with medial compartment osteoarthritis of the knee. J Rheumatol. 2001;28(12):2705-10.

18. Russell EM, Hamill J. Lateral wedges decrease biomechanical risk factors for knee osteoarthritis in obese women. J Biomech. 2011;44(12):2286-91. doi:10.1016/j.jbiomech.2011.05.033

19. Mølgaard CM, Graven-Nielsen T, Simonsen O, Kersting UG. Potential interaction of experimental knee pain and laterally wedged insoles for knee off-loading during walking. Clin Biomech Bristol Avon. 2014;29(8):848-54. doi:10.1016/j.clinbiomech.2014.08.002

20. Hajizadeh M, Desmyttere G, Carmona JP, Bleau J, Begon M. Can foot orthoses impose different gait features based on geometrical design in healthy subjects? A systematic review and meta-analysis. Foot Edinb. 2020;42:101646. doi:10.1016/j.foot.2019.10.001

21. Stacoff A, Reinschmidt C, Stüssi E. The movement of the heel within a running shoe. Med Sci Sports Exerc. 1992;24(6):695-701.

22. Visual3D Wiki. Temporal distance calculations for gait [Internet]. C-Motion Inc; 2021 [cited 2021 May 2]. Available from: https://c-motion.com/v3dwiki/index.php?title=Temporal_Distance_Calculations_for_Gait

23. Carson MC, Harrington ME, Thompson N, O'Connor JJ, Theologis TN. Kinematic analysis of a multi-segment foot model for research and clinical applications: a repeatability analysis. J Biomech. 2001;34(10):1299-307. doi:10.1016/s0021-9290(01)00101-4

24. Wright CJ, Arnold BL, Coffey TG, Pidcoe PE. Repeatability of the modified Oxford foot model during gait in healthy adults. Gait Posture. 2011;33(1):108-12. doi:10.1016/j.gaitpost.2010.10.084

25.   Oxford Foot Model [Internet]. NHS Foundation Trust; 2021 [cited 2021 May 6]. Available from: https://www.ouh.nhs.uk/gait-lab/research/oxford-foot-model.aspx

26.   Levinger P, Murley GS, Barton CJ, Cotchett MP, McSweeney SR, Menz HB. A comparison of foot kinematics in people with normal- and flat-arched feet using the Oxford Foot Model. Gait Posture. 2010;32(4):519-23. doi:10.1016/j.gaitpost.2010.07.013

27.   McCahill J, Stebbins J, Koning B, Harlaar J, Theologis T. Repeatability of the Oxford Foot Model in children with foot deformity. Gait Posture. 2018;61:86-9. doi:10.1016/j.gaitpost.2017.12.023

28.   Stebbins J, Harrington M, Thompson N, Zavatsky A, Theologis T. Gait compensations caused by foot deformity in cerebral palsy. Gait Posture. 2010;32(2):226-30. doi:10.1016/j.gaitpost.2010.05.006

29.   Tekscan. The gait cycle: phases, parameters to evaluate & technology [Internet]. 2021 [cited 2021 May 7]. Available from: https://www.tekscan.com/blog/medical/gait-cycle-phases-parameters-evaluate-technology

30.   Moon D, Esquenazi A. Instrumented Gait Analysis: A Tool in the Treatment of Spastic Gait Dysfunction. JBJS Rev. 2016;4(6):e4 . doi:10.2106/JBJS.RVW.15.00076

31.   Eng JJ, Winter DA. Kinetic analysis of the lower limbs during walking: what information can be gained from a three-dimensional model? J Biomech. 1995;28(6):753-8. doi:10.1016/0021-9290(94)00124-m

32.   Murray MP, Mollinger LA, Gardner GM, Sepic SB. Kinematic and EMG patterns during slow, free, and fast walking. J Orthop Res. 1984;2(3):272-80. doi:10.1002/jor.1100020309

33.   Gorton GE 3rd, Hebert DA, Gannotti ME. Assessment of the kinematic variability among 12 motion analysis laboratories. Gait Posture. 2009;29(3):398-402. doi:10.1016/j.gaitpost.2008.10.060

34.   Alcantara RS, Trudeau MB, Rohr ES. Calcaneus range of motion underestimated by markers on running shoe heel. Gait Posture. 2018;63:68-72. doi:10.1016/j.gaitpost.2018.04.035